

Monoclonal Antibodies Identify a Group of Nuclear Pore Complex Glycoproteins

Claudette M. Snow, Alayne Senior, and Larry Gerace

Department of Cell Biology and Anatomy, The Johns Hopkins University School of Medicine, Baltimore, Maryland 21205

Abstract. Using monoclonal antibodies we identified a group of eight polypeptides of rat liver nuclear envelopes that have common epitopes. Most or all of these proteins are structurally distinct, as shown by tryptic peptide mapping and analysis with polyclonal antibodies. While these polypeptides are relatively tightly bound to nuclear membranes, only one is an integral membrane protein. The eight antigens cofractionate with the nuclear pore complex under various conditions of ionic strength and detergent. It can be seen by immunofluorescence microscopy that the monoclonal antibodies reacting with these antigens stain the nuclear surface of interphase cells in a finely punctate pattern. When the nuclear envelope is disassembled and subsequently reformed during mitosis, the proteins are reversibly dispersed throughout the

cytoplasm in the form of minute foci. By EM immunogold localization on isolated nuclear envelopes, the monoclonal antibodies label exclusively the nuclear pore complex, at both its nucleoplasmic and cytoplasmic margins. Considered together, our biochemical and localization data indicate that the eight nuclear envelope polypeptides are pore complex components. As shown in the accompanying paper (Holt, G. D., C. M. Snow, A. Senior, R. S. Haltiwanger, L. Gerace, and G. W. Hart, *J. Cell Biol.*, 104:1157-1164) these eight polypeptides contain a novel form of glycosylation, O-linked *N*-acetylglucosamine. The relative abundance and disposition of these O-linked glycoproteins in the pore complex are consistent with their having a role in nucleocytoplasmic transport.

THE nuclear envelope forms the membrane boundary of the nucleus in eukaryotic cells (for reviews see references 13 and 14). Its principal functions include compartmentalization of nuclear metabolism and control of selective macromolecular movement between nucleus and cytoplasm. The major structural components of the nuclear envelope are inner and outer nuclear membranes, nuclear lamina, and pore complexes. The nuclear lamina (reviewed in references 16 and 33) is a meshwork of intermediate filaments lining the nucleoplasmic surface of the inner nuclear membrane, which is thought to provide a framework for the regulation of nuclear envelope structure and an anchoring site at the nuclear periphery for interphase chromosomes (18). Pore complexes constitute large supramolecular structures present at regions where inner and outer nuclear membranes are joined to form pores (2, 15), and are thought to be the major or exclusive sites of molecular exchanges across the nuclear envelope (1, 13, 14, 39).

Based on cell microinjection studies, the pore complex appears to contain an aqueous channel of ~ 10 nm in diameter through which solutes and sufficiently small macromolecules (e.g., proteins <20 – 40 kD) can migrate by passive diffusion (35, 41). However, nucleocytoplasmic transport of larger macromolecules probably involves mediated mechanisms (7, 10). Recent work has shown that certain nuclear proteins contain discrete structural regions (6) or sequences

(21, 23, 28, 36) that mediate their nuclear localization. While the mechanism of action of these localization sequences is not clearly established, they may interact specifically with components of the nuclear pore complex to mediate nuclear import.

Understanding the processes of nucleocytoplasmic transport will require detailed biochemical information on the pore complex. This structure may have a molecular weight of 25 – 50×10^6 , but relatively little is known about its macromolecular constituents. At least most of the pore complex consists of protein (1, 8), but up to now only two of its polypeptides have been identified. One of these (gp190) is an integral membrane glycoprotein of 190 kD (19) apparently containing high-mannose oligosaccharide (3, 19), which may anchor the pore complex to nuclear membranes. A second pore complex glycoprotein of 62 kD was described recently (5) that binds wheat germ agglutinin (a lectin specific for *N*-acetylglucosamine and sialic acids).

To obtain immunological probes specific for the pore complex, we isolated a number of monoclonal antibodies reacting with rat liver nuclear envelopes. Using these antibodies, we identified a group of eight structurally distinct nuclear envelope polypeptides that share epitopes. Based on subcellular fractionation and immunocytochemical localization, these polypeptides occur specifically in the nuclear pore complex. As shown in the accompanying paper (25), the

common epitopes of these proteins contain a recently-described type of glycosylation, O-linked *N*-acetylglucosamine (24, 44). Based on our localization results, this unusual sugar linkage is cytoplasmically disposed, in contrast to the luminal disposition of other well-characterized protein glycosylation of intracellular membrane compartments. The possible involvement of these glycoproteins in nucleocytoplasmic transport is discussed.

Materials and Methods

Isolation and Fractionation of Nuclear Envelopes

Unless otherwise noted, all procedures described in Materials and Methods were conducted at 0–4°C. Nuclear envelopes were isolated from rat liver as described (18). 1 U of nuclear envelopes is the amount derived from 1 A₂₆₀ U of isolated rat liver nuclei (containing 3×10^6 nuclei). To prepare salt-washed nuclear envelopes, pellets of crude nuclear envelopes were resuspended in 10% sucrose, 10 mM triethanolamine-HCl, pH 7.4, 0.1 mM MgCl₂, and 1 mM dithiothreitol (DTT) (STM buffer)¹ at a concentration of ~1.5 mg/ml protein, and to this was added an equal volume of STM buffer containing 1 M NaCl. After 5 min, the sample was centrifuged over a cushion of STM buffer containing a total of 30% sucrose for 20 min at 6,500 *g* in a centrifuge (J6B; Beckman Instruments, Inc., Palo Alto, CA).

For various chemical extractions, pellets of crude or salt-washed nuclear envelopes (see Fig. 6) were resuspended at a concentration of ~0.75 mg/ml protein in (a) STM buffer containing 2 M NaCl; (b) 10% sucrose, 2% Triton X-100, 20 mM triethanolamine-HCl, pH 7.4, 20 mM KCl, 5 mM MgCl₂, and 1 mM DTT (Triton/low salt buffer); (c) 10% sucrose, 2% Triton X-100, 20 mM MES-KOH, pH 6.0, 300 mM KCl, 2 mM EDTA, and 1 mM DTT (Triton/high salt buffer); (d) 0.1 N NaOH, and 10 mM DTT; or (e) 4 M guanidine-HCl, 50 mM triethanolamine-HCl, pH 7.4, and 10 mM DTT. Samples were incubated for 5 min (a, d, and e) or for 30 min (b and c) and were centrifuged for 30 min at 6,500 *g* in a J6B centrifuge (a–c) or for 1 h at 140,000 *g* in a 50 Ti rotor (d and e) to yield supernatants and pellets (centrifuge and rotor, Beckman Instruments, Inc.).

Production and Characterization of Monoclonal and Polyclonal Antibodies

To obtain monoclonal antibodies, a pore complex–lamina fraction isolated from rat liver nuclear envelopes by sequential extraction with 1 M NaCl and 2% Triton X-100 in low ionic strength buffer (8) was used to immunize 18–19-wk-old BALB/c mice (Harlan Sprague Dawley, Inc., Indianapolis, IN). The initial injection involved 750 µg protein in complete Freund's adjuvant (administered intraperitoneally and subcutaneously), followed by two to three subsequent injections given at 4–5-wk intervals with 150 µg protein in incomplete Freund's adjuvant (administered in the same fashion). Approximately 1 mo after the penultimate injection, mice were injected intraperitoneally with 150–450 µg protein in PBS (10 mM sodium phosphate, pH 7.4, 140 mM NaCl), and 3 d later were killed. Spleen cells from immunized mice were then fused with the mouse myeloma cell line P3-X63-Ag8.653 (30) and hybridomas were grown as described (31). Culture supernatants from fusion wells were screened by immunoblot analysis of salt-washed rat liver nuclear envelopes and by immunofluorescence microscopy of normal rat kidney (NRK) cells (see below). Fusion wells that yielded an appropriate positive reaction with both assays were subcloned two successive times in soft agar (31) or by limiting dilution in 96-well microtiter plates using mouse thymocytes as a feeder layer. Freezing of myeloma lines and production of ascites fluid in mice was carried out as described (31).

Monoclonal IgGs were purified by DEAE cellulose column chromatography (47). Pooled peak fractions were dialyzed against 50% glycerol in PBS and stored at –20°C. Monoclonal IgMs were isolated by centrifuging ascites fluid at 140,000 *g* for 15 min and chromatographing the supernatant on a column of Sephacryl S-400 in a buffer containing 50 mM Tris-HCl, pH 8.8, 500 mM NaCl, and 0.02% NaN₃. IgM peak fractions from the column were pooled, concentrated to 1 mg/ml, and dialyzed against 50% glycerol, 25 mM Tris-HCl, pH 8.0, 250 mM NaCl, and 0.01% NaN₃ and stored at –20°C.

1. *Abbreviations used in this paper:* NRK, normal rat kidney; STM buffer, 10% sucrose, 10 mM triethanolamine-HCl, pH 7.4, 0.1 mM MgCl₂, and 1 mM DTT.

The isotype of each monoclonal antibody was determined as described (27). Isotypes of antibodies used in this study are RL1, IgM; RL2, IgG1; RL3, IgG1; RL4, IgG1; RL6, IgG3; RL11, IgG1; and RL12, IgM. For control mouse monoclonal antibodies, an irrelevant monoclonal IgG1 (HA4) (27) was the kind gift of Dr. Ann Hubbard, and an irrelevant monoclonal IgM (MSI) was kindly provided by Dr. Mette Strand, both of Johns Hopkins University School of Medicine.

To prepare polyclonal antibodies to individual glycoprotein polypeptides, antigens were immunoadsorbed from nuclear envelopes with RL2 conjugated to Sepharose 4B (see below), and proteins were electrophoresed on preparative SDS gels. Individual bands were excised from these gels after staining in aqueous Coomassie Blue (0.1% Coomassie Blue in 25 mM Tris base, 190 mM glycine), were homogenized in H₂O and were injected into 4–6-lb New Zealand white rabbits. The first immunization (~20–40 µg protein) was in complete Freund's adjuvant and was administered by multiple site injections. Booster injections (~10–20 µg protein) were given at ~1–2-mo intervals in incomplete Freund's adjuvant at multiple sites. Antibodies raised against specific bands were affinity purified using nitrocellulose transfers of the same bands as immunoadsorbents (4).

Binding Studies with Monoclonal Antibodies

Solid-phase competitive binding analysis with monoclonal antibodies was done essentially as described (31). The 180-kD glycoprotein was immunoadsorbed from rat liver nuclear envelopes with antibody RL11 (below). Antigens were eluted from immunoadsorbent beads with 0.5% SDS, 10 mM ammonium acetate, pH 8.0, and this eluate was diluted to 0.01% SDS before being dried in 96-well microtiter plates (40 ng of the 180-kD polypeptide applied per well). Antibodies were labeled with ¹²⁵I by the chloramine T procedure to specific activities of 6–15 × 10⁶ cpm/µg (22) and were incubated in microtiter wells at a concentration of 1–3 × 10^{–9} M in the presence or absence of a 1,000-fold molar excess of various unlabeled monoclonal antibodies.

For quantitative analysis of binding of antibodies to isolated nuclear envelopes, monoclonal antibodies labeled with ¹²⁵I (22) were diluted to a specific activity of 1.6 × 10⁶ cpm/µg with unlabeled antibodies. Salt-washed rat liver nuclear envelopes (0.45 mg/ml) were then incubated for 90 min using gentle agitation with various concentrations of monoclonal antibodies in a buffer containing 2 mg/ml bovine serum albumin (fraction V; Miles Scientific Div., Naperville, IL), 25 mM triethanolamine-HCl, pH 7.4, 125 mM NaCl, and 1 mM MgCl₂. Samples (50 µl) were then layered over a 200-µl cushion of 20% sucrose, 10 mM triethanolamine-HCl, pH 7.4, and 0.1 mM MgCl₂ in 400 µl (5-cm long) polyethylene tubes and were centrifuged at 15,000 *g* for 10 min to pellet nuclear envelopes and bound antibody. Supernatants and pellets were then counted in a gamma counter. Nonspecific antibody binding was measured by incubating nuclear envelopes with ¹²⁵I-labeled HA4. All samples were analyzed in triplicate.

Gel Electrophoresis and Peptide Mapping

SDS PAGE of proteins was carried out on 7.5–15% gradient gels (38) using the sample preparation conditions described (19). Apparent molecular masses of proteins were determined from their mobilities on a 7% SDS polyacrylamide gel compared with high molecular mass protein standards (myosin, 205 kD; β-galactosidase D, 116 kD; phosphorylase B, 97.4 kD; bovine serum albumin, 66 kD; and egg albumin, 45 kD; Sigma Chemical Co., St. Louis, MO). Mass of protein bands on Coomassie Blue–stained SDS gels was determined by dye elution in 25% pyridine followed by spectrophotometric measurement of 605 nm (12) using bovine serum albumin as a standard. Two-dimensional gel separation involved electrophoresis on nonequilibrium pH gradient gels followed by SDS polyacrylamide gels as described (40). Two-dimensional tryptic peptide mapping on cellulose thin-layer plates was carried out as described (9) with modifications (26).

Immunoblotting

For immunoblotting, proteins on one- or two-dimensional SDS gels were electrophoretically transferred to sheets of nitrocellulose paper (Schleicher & Schuell, Inc., Keene, NH) as described (19). Blots were sometimes stored in PBS for up to 2 mo. Transferred proteins were visualized by staining the nitrocellulose sheets in 0.2% Ponceau S, 3% trichloroacetic acid followed by destaining in H₂O. Immediately before antibody labeling, the blots were incubated at 70°C for 1 h in PBS (Dr. Velia Fowler, Harvard University, Cambridge, MA, personal communication). This heat treatment was necessary to obtain reproducibly high levels of labeling of all antigen bands on immunoblots with the monoclonal antibodies. After an initial incubation for

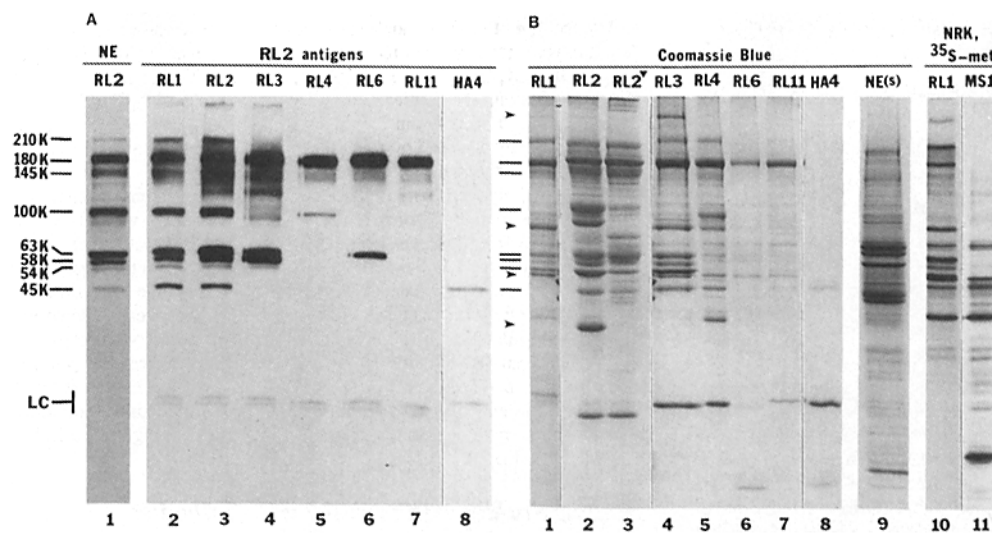


Figure 1. Immunoblotting characterization of monoclonal antibodies recognizing eight related nuclear envelope polypeptides. (A) Samples of total salt-washed rat liver nuclear envelopes (lane 1, 4 U loaded) or of the antigens immunoadsorbed by RL2 (lanes 2–8, protein adsorbed from 20 U of nuclear envelopes loaded per lane) were analyzed by immunoblotting with various monoclonal antibodies, including an irrelevant monoclonal IgG (HA4). Note that the 210- and 45-kD bands were labeled more strongly on immunoblots by RL2 relative to the other bands when greater quantities of antigen were loaded per gel

lane (cf. lanes 1 and 3). Molecular mass designations to the left of lane 1 indicate the eight major immunoblot-reactive bands. (B, lanes 1–8), Salt-washed rat liver nuclear envelopes were solubilized (see Materials and Methods) in either Triton/high salt buffer (lanes 1, 2, and 4–8) or in SDS buffer (lane 3) and were immunoadsorbed with various monoclonal antibodies conjugated to Sepharose 4B. Bound samples were then subjected to electrophoresis on SDS gels and stained with Coomassie Blue. Polypeptides adsorbed by monoclonal antibodies that react with various subsets of the eight nuclear envelope polypeptides (lanes 1–7) or by an irrelevant monoclonal IgG (lane 8) are shown. The salt-washed nuclear envelope protein used for immunoadsorption [NE(s)] is shown in lane 9 (5 U loaded). Immunoadsorbed material from 300 U (lanes 1 and 4–8) or 200 U (lanes 2 and 3) of nuclear envelopes were loaded (40–60 times the amount of lane 9). The experiment in lanes 2 and 3 was run on a different gel from the experiments of remaining lanes, and the 210-, 100-, and 87-kD polypeptides of these two gels cannot be precisely aligned. Only antibody RL2 quantitatively adsorbed all of its immunoblot-reactive polypeptides (lane 2) from Triton/high salt-solubilized samples. The four arrowheads to the left of lane 1 denote additional major bands migrating at 250, 87, 52, and 41 kD that appeared in some immunoadsorbed samples but that were not recognized on immunoblots (A). The migration position of immunoglobulin light chain (LC) is shown. (Lanes 10 and 11) NRK cells were labeled with [³⁵S]methionine for 15 h, solubilized in Triton/high salt buffer, and 15,000 g supernatants of solubilized cells were used for immunoadsorption by either RL1 (an IgM) or by an irrelevant monoclonal IgM (MS1) to determine nonspecific background. Shown is a fluorograph of an SDS gel of the adsorbed samples. From this biosynthetically labeled sample, RL1 specifically immunoadsorbed bands at 250, 210, 180, 145, 87, 63, 58, and 54 kD.

30 min at room temperature in 0.5% Triton X-100, 2% bovine serum albumin (fraction V; Miles Scientific Div.) in PBS, blots were given sequential 1-h incubations at room temperature with 5 µg/ml mouse monoclonal antibody followed by 10⁶ cpm/ml ¹²⁵I-rabbit anti-mouse IgG in the Triton/bovine serum albumin/PBS solution. Blots were given five 5-min washes in 0.5% Triton X-100 in PBS after each of these two antibody incubations. Alternately, blots were incubated (and subsequently washed) sequentially in 5 µg/ml mouse monoclonal antibody, 1 µg/ml rabbit anti-mouse IgG, and, finally, 10⁶ cpm/ml ¹²⁵I-protein A as described above. Immunoblots were air-dried and exposed to x-ray film for autoradiography at –80°C using a Lightning Plus intensifying screen (E. I. Dupont de Nemours & Co., Wilmington, DE). Rabbit anti-mouse IgG and protein A were iodinated to specific activities of ~7 × 10⁶ and 10⁸ cpm/µg, respectively, by the chloramine T procedure (22).

Immunoadsorption

Purified monoclonal antibodies were conjugated to cyanogen bromide-activated Sepharose 4B (Pharmacia Fine Chemicals, Piscataway, NJ) at a concentration of 5 mg/ml in a buffer containing 0.2 M sodium carbonate, pH 8.9, according to the manufacturer's instructions. To solubilize nuclear envelope proteins for immunoadsorption, pellets of salt-washed nuclear envelopes were resuspended at a protein concentration of 0.75 mg/ml in 2% Triton X-100, 20 mM Tris, pH 8.8, 500 mM NaCl, 2 mM EDTA, 0.5 mM phenylmethylsulfonyl fluoride (PMSF), 1% trasyolol, and 2 µg/ml each of chymostatin, leupeptin, antipain, and pepstatin A. After sonication and incubation for 1 h, samples were centrifuged for 15 min at 15,000 g in a microfuge, and supernatants were mixed with an equal volume of the above solubilization buffer containing 45 mM Hepes-KOH, pH 6.8, instead of 20 mM Tris, pH 8.8. Subsequently, samples were incubated overnight with monoclonal antibodies conjugated to Sepharose 4B (usually 20 µl of antibody-bead conjugate per 150 µg solubilized nuclear envelope protein).

Beads were then washed four times with 2% Triton X-100, 30 mM Tris-HCl, pH 7.4, 500 mM NaCl, and 2 mM EDTA and two times with 10 mM Tris-HCl, pH 7.4. Finally, antigens were eluted from immunoadsorbent beads in SDS gel sample buffer (17).

In some immunoadsorption experiments, nuclear envelopes were solubilized at 0.25 mg/ml by boiling in 0.2% SDS, 50 mM triethanolamine-HCl, pH 7.4, 100 mM NaCl, 2 mM EDTA, 0.5 mM PMSF, and 2 µg/ml each of chymostatin, leupeptin, antipain, and pepstatin A. After cooling, Triton X-100 was added to 2% and samples were centrifuged at 15,000 g for 15 min. Supernatants were then incubated with antibody-Sepharose conjugates for immunoadsorption as described above.

Immunolocalization

For immunofluorescence microscopy of tissue culture cells, NRK cells were grown on glass coverslips in Dulbecco's modified Eagle's medium (Gibco, Grand Island, NY) containing 10% fetal calf serum, 100 U/ml penicillin, and 100 µg/ml streptomycin. Cells were fixed by incubating coverslips for either 4 or 10 min at room temperature in 4% paraformaldehyde in PBS containing 0.1 mM MgCl₂ and 0.1 mM CaCl₂. Cells were then permeabilized with 0.5% Triton X-100 in PBS and labeled for indirect immunofluorescence microscopy as described (46). The fluorescent antibody was rhodamine-conjugated rabbit anti-mouse IgG (Cappel Worthington Biochemicals, Malvern, PA).

For immunofluorescence labeling of liver cryosections, fresh rat liver was diced into small cubes and immediately frozen in O.C.T. embedding compound (Miles Scientific Div.) in a bath of isopentane cooled in liquid N₂. 4-µm cryosections were then cut, mounted on glass slides, fixed in 100% methanol at 0°C for 10 min, and processed for immunofluorescence staining as described above.

EM immunogold localization was performed on salt-washed rat liver nuclear envelopes. First, 0.15 mg/ml suspensions of nuclear envelopes in STM

Table I. Specificity of Monoclonal Antibodies Revealed by Immunoblot Analysis*

monoclonal antibody	210 kD	180 kD	145 kD	100 kD	63 kD	58 kD	54 kD	45 kD
RL1	+	+	+	+	+	+	+	+
RL2	+	+	+	+	+	+	+	+
RL3	-	+	+	-	+	+	+	-
RL4	-	+	-	+	-	-	-	-
RL6	-	+	-	-	+	-	-	-
RL11	-	+	-	-	-	-	-	-

* Taken from Fig. 1 A. Antibodies RL2 and RL3 also reacted with bands in the 90–145 kD range. Since no major bands in this region were immunoadsorbed by the same antibodies, these immunoreactive bands were not further characterized.

buffer were pipetted into plastic tissue culture petri dishes that were centrifuged at 500 g for 15 s in a J6B centrifuge to attach the nuclear envelopes to the petri dishes, where all subsequent processing occurred. Material was then given an initial fixation in 4% paraformaldehyde in PBS for 10 min at room temperature, and subsequently incubated in 50 mM NH₄Cl in PBS for 10 min. Next, samples were incubated in a humid chamber for 30–60 min at room temperature with various monoclonal antibodies diluted to a concentration of 14–50 µg/ml in PBS containing 0.2% gelatin. After washing in PBS, samples were incubated in a humid chamber with goat anti-mouse IgM or goat anti-mouse IgG conjugated with 5 nm gold (Janssen Life Sciences Products, Piscataway, NJ) for 0.5–4 h at room temperature or 6–18 h at 4°C. After more washes in PBS, samples were fixed in 2% glutaraldehyde, 0.2% tannic acid in PBS containing 0.1 mM MgCl₂, and were further postfixed in OsO₄, embedded, sectioned, and stained for EM as described (19).

Results

A Group of Nuclear Envelope Polypeptides Identified by Monoclonal Antibodies

A pore complex-enriched subfraction of rat liver nuclear envelopes was used to prepare a number of mouse monoclonal antibodies. In immunofluorescence staining of cultured cells (see below), some antibodies gave distinct punctate labeling of the nuclear surface. This class of antibodies was selected for analysis in this paper. Surprisingly, on immunoblots of nuclear envelope protein all of these antibodies reacted with specific subsets of a group of eight different nuclear envelope polypeptides with apparent molecular masses of 210, 180, 145, 100, 63, 58, 54, and 45 kD (Fig. 1 A and Table I).² Some monoclonal antibodies (e.g., RL1 and RL2) reacted with all eight polypeptides, while other monoclonals reacted with smaller subsets of the group (Table I). Every antibody bound to the 180-kD band, and one antibody (RL11) was virtually monospecific for this polypeptide. Identical sets of bands were labeled on immunoblots by each antibody when either total nuclear envelope protein (Fig. 1 A, lane 1 for RL2; remainder not shown) or the nuclear envelope antigens immunoadsorbed by monoclonal antibody RL2 (Fig. 1 A, lanes 2–8) were analyzed.

The monoclonal antibodies also were characterized by immunoadsorption of antigens from solubilized rat liver nuclear envelopes followed by analysis on SDS gels (Fig. 1 B,

2. Several additional polypeptides between 90 and 145 kD also were recognized on immunoblots by monoclonal antibodies RL2 and RL3 [see Fig. 1 A, lanes 3 and 4], but since these bands represented minor stained species in immunoadsorbed samples [Fig. 1 B], they were not included in our analysis. In contrast, while the 54 and 45 kD bands were labeled only weakly on immunoblots, they corresponded to relatively major polypeptides in immunoadsorbed samples [see Fig. 2] and were therefore included in our study.

lanes 1–8). Typically, all of the bands recognized on immunoblots by a particular monoclonal antibody were adsorbed (with greater or lesser efficiency) by the same antibody, as shown by immunoblot analysis of the adsorbed and unadsorbed protein fractions (data not shown) and by the presence of major bands in immunoprecipitates that precisely comigrated with the major labeled polypeptides on immunoblots (cf. Figs. 1, A and B; see also Fig. 2 below). Bands of similar migration to the polypeptides detected on immunoblots of rat liver nuclear envelopes by RL1 were specifically adsorbed by this antibody from NRK cells labeled for 15 h with ³⁵S-methionine (Fig. 1 B, cf. lanes 10, 11, and 1), showing that rapidly dividing cells also express these polypeptides.

A Triton/high salt buffer commonly was used for nuclear envelope solubilization in these experiments, since it permitted efficient immunoadsorption. However, with this relatively nondenaturing condition, additional polypeptides not

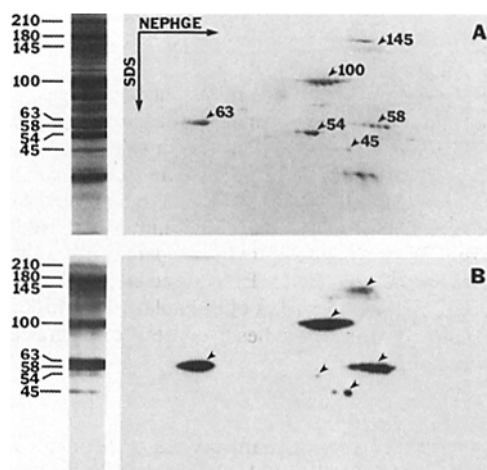


Figure 2. Two-dimensional gel analysis of the nuclear envelope antigens recognized by monoclonal antibodies. The RL2 antigens were immunoadsorbed from nuclear envelopes solubilized in Triton/high salt buffer. Adsorbed samples were then subjected to non-equilibrium pH gradient electrophoresis (NEPHGE) followed by SDS gel electrophoresis (SDS). Two-dimensional gels were either stained with Coomassie Blue (A) or were analyzed by immunoblotting with RL2 (B). Samples of the proteins adsorbed by RL2 were run on the SDS gel as standards (lanes at left of A and B; molecular masses designate RL2-immunoreactive bands). Arrowheads in A and B indicate the six immunoreactive bands present in RL2 immunoprecipitates that were clearly resolved on the two-dimensional gels.

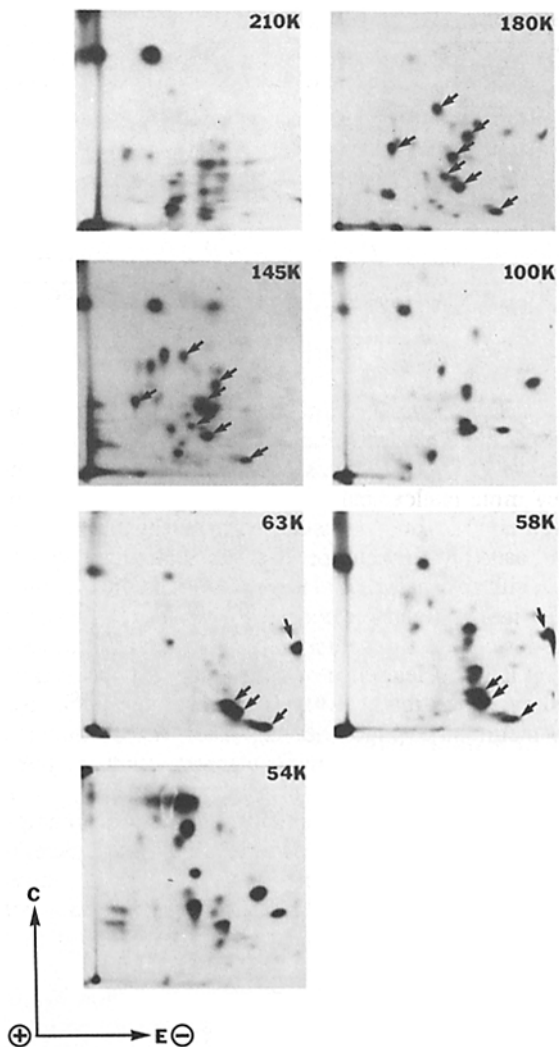


Figure 3. Tryptic peptide mapping of the related nuclear envelope antigens. The RL2 antigens were immunoadsorbed from nuclear envelopes that had been solubilized in Triton/high salt buffer and were subjected to electrophoresis on an SDS gel. After staining with Coomassie Blue, bands at 210, 180, 145, 100, 63, 58, and 54 kD were separately excised, iodinated with chloramine T, and limit-digested with trypsin. Tryptic digests were then separated on cellulose thin-layer plates by electrophoresis (E) followed by chromatography (C). The origin is at the lower left of each plate. The 45-kD antigen was not analyzed in these studies because it co-migrated with the heavy chain of IgG.

detectable on immunoblots by any antibodies were specifically present in many immunoadsorbed samples, including members of a group of four major polypeptides migrating at 250, 87, 52, and 41 kD (Fig. 1 B, arrowheads to left of lane 1) as well as a number of more minor bands. The major polypeptides apparently do not directly react with the monoclonal antibodies (Fig. 1; see accompanying paper [25]) and probably coprecipitate with the monoclonal-specific antigens due to a noncovalent physical association with the latter that is not disrupted in Triton/high salt buffer. In support of this possibility, when nuclear envelopes were first solubilized in SDS to disrupt noncovalent protein interactions before immunoadsorption, the two major bands at 87 and 41 kD in samples adsorbed by RL2 from Triton-high salt-sol-

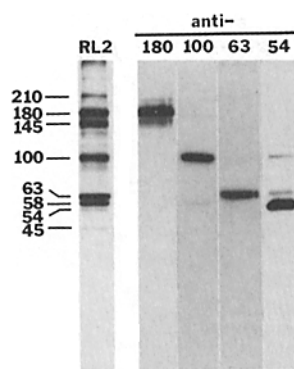


Figure 4. Immunoblot analysis of the related nuclear envelope antigens with polyclonal antibodies. The nuclear envelope polypeptides adsorbed by RL2 were analyzed by immunoblotting with monoclonal antibody RL2, or with affinity-purified polyclonal antibodies prepared against the 180-, 100-, 63-, and 54-kD bands.

ubilized material were absent (Fig. 1 B, cf. lanes 2 and 3), although adsorption of some immunoreactive bands (especially the 100- and 54-kD species) was less efficient with this condition.

The nuclear envelope proteins immunoadsorbed by RL2 were also examined by electrophoresis on 2-D gels (Fig. 2), where it was possible to detect all polypeptides except for the high molecular mass (the 210 and 180 kD) polypeptides which were not clearly resolved in the first dimension. The bands of 145, 100, 63, 58, 54, and 45 kD each gave rise to a single major species (usually consisting of multiple charge isoforms) on 2-D gels stained with Coomassie Blue (Fig. 2 A, arrows) or with silver (data not shown). Each of these co-migrated with a single immunoreactive species having the same molecular mass and charge isoforms (Fig. 2 B). Thus, most of protein mass in the bands found at these molecular mass positions in immunoadsorbed samples is contributed by single polypeptides that directly react with our monoclonal antibodies.

Structurally Distinct Polypeptides with Multiple Common Epitopes

To examine whether the set of immunologically related polypeptides recognized by our monoclonal antibodies could arise from a common precursor(s) by proteolytic cleavage, we analyzed the polypeptides by two-dimensional tryptic peptide mapping after chemical iodination (Fig. 3). Unique maps were found for all members of the set comprising the 210-, 180-, 100-, 63-, and 54-kD species. In addition, the pairs consisting of the 180/145-kD bands and the 63/58-kD bands shared labeled peptides (Fig. 3, arrows). Since the band migrating more quickly of each of these two pairs contained four to eight strongly labeled unique peptides, it probably did not arise by simple proteolytic cleavage of the species migrating more slowly. In the case of the 180/145-kD pair, the 145-kD band may be contaminated with proteolytic products of the upper band, since the 180-kD band is very sensitive to degradation by various proteases *in vitro* (data not shown). However, most of the 145-kD band must be a unique species since it (but not the 180-kD band) contains an integral membrane protein (see below).

To further examine the relationships among members of this set of polypeptides, we prepared polyclonal rabbit antisera to the bands of 180, 100, 63, and 54 kD excised from SDS gels of immunoadsorbed samples. Affinity-purified polyclonal antibodies were then used for analysis of the RL2 antigens on immunoblots (Fig. 4). Each polyclonal antibody

		¹²⁵ I-labeled monoclonal antibodies				
		RL1	RL2	RL3	RL11	RL6
Unlabeled monoclonal antibodies	RL1	2	68	45	49	57
	RL2	40	3	59	90	110
	RL3	26	76	0	2	93
	RL11	57	94	80	1	130
	RL4	54	89	123	80	129
	HA4	104	108	98	87	94

Figure 5. Competitive solid-phase binding of various monoclonal antibodies to the 180-kD polypeptide. The 180-kD polypeptide was immunopurified from rat liver nuclear envelopes with monoclonal antibody RL11 conjugated to Sepharose 4B and was adsorbed to plastic microtiter dishes. Subsequently, binding of ¹²⁵I-labeled monoclonal antibodies to the antigen was measured in the absence or presence of a 10³-fold excess of various unlabeled monoclonal antibodies, including an irrelevant monoclonal IgG (HA4). Numbers represent the percent of the control binding (i.e., binding achieved in the absence of competitor) of various labeled antibodies (top) that was obtained when various unlabeled antibodies (left) were present. Instances where <5% labeled antibody binding was obtained are shown in bold numbers. This competition analysis did not include labeled RL4, which reacted poorly with the immobilized antigen, and unlabeled RL6.

(presumably recognizing many epitopes) bound predominantly to a single band at the expected molecular mass, although the anti-180-kD antibody also labeled a series of minor quickly migrating species in the 150–180 kD region of the gel (see above). Thus, in contrast to the monoclonal antibodies, the polyclonal antibodies primarily recognized epitopes not shared among the eight proteins. Taken together with the peptide mapping data, these results indicate that most or all of the eight polypeptides are structurally distinct species that do not arise by proteolytic processing of other members of the group.

We used solid-phase competition binding to investigate whether the 180-kD polypeptide contains spatially separated epitopes recognized by the different monoclonal antibodies, or whether the epitopes all occur at or near the same site. The binding of various ¹²⁵I-labeled monoclonal antibodies to the affinity-purified protein was measured in the presence or absence of a large excess of each of the other unlabeled antibodies (Fig. 5). In almost all cases examined, only the homologous unlabeled antibody resulted in >95% inhibition of binding of each labeled antibody. The heterologous antibodies inhibited binding weakly (usually by <50%) or not at all. Qualitatively very similar results were obtained when the whole group of antigens immunoadsorbed by antibody

RL2 were analyzed by the competitive binding assay (data not shown). We conclude that at least the 180-kD polypeptide appears to contain multiple spatially separated epitopes recognized by our set of monoclonal antibodies. These results are readily understood in terms of the chemical characteristics of these epitopes, which involve a protein glycosylation site (see accompanying paper [25]).

Cofractionation of the Proteins with the Pore Complex

We used immunoblot analysis to follow the fractionation of the RL1 antigens upon extraction of isolated rat liver nuclei or nuclear envelopes with a variety of enzymatic and chemical conditions (Fig. 6).³ When nuclei were digested with DNase and RNase in a low ionic strength buffer to release the nuclear contents from crude nuclear envelopes (references 8 and 29; Fig. 6 B, lanes 2 and 3), most of the mass of all detectable nuclear envelope antigens occurred in the nuclear envelope pellet and was not extracted (Fig. 6 A, lanes 2 and 3), similar to the behavior of nuclear lamins (data not shown).

Extraction of crude nuclear envelopes (Fig. 6 B, lane 4) with 0.5 M NaCl leads to solubilization of most histones and other chromatin proteins from tightly bound nuclear envelope components (reference 20; Fig. 6 B, lanes 5 and 6). With this treatment, most of the mass of the detectable antigens appeared in the nuclear envelope pellet (Fig. 6 A, lanes 5 and 6). Even upon extraction of nuclear envelopes with 2 M NaCl (conditions that result in partial structural disruption of pore complex; see reference 45), >50% of all detectable antigens occurred in the pellet fraction (Fig. 6 A, lanes 7 and 8), although the 180-, 63-, and 58-kD bands were extracted more extensively than the other bands by this treatment.

When nuclear envelopes are extracted with Triton X-100 in a low ionic strength buffer, nuclear membranes and integral membrane proteins of the outer nuclear membrane (e.g., cytochrome p450) are solubilized, while the pore complex remains structurally intact and the pore complex marker protein gp190 is found in the pellet fraction with the lamins (reference 19; Fig. 6 B, lanes 9 and 10). Similarly, the antigens recognized by our monoclonal antibodies quantitatively pelleted after the low ionic strength Triton extraction (Fig. 6 A, lanes 9 and 10). In contrast, extraction of nuclear envelopes with Triton X-100 in higher salt (0.3 M KCl) leads to selective solubilization of pore complexes and gp190, while the lamins remain insoluble and pellet (references 19 and 20; Fig. 6 B, lanes 11 and 12). Extraction of nuclear envelopes with this high salt Triton condition resulted in complete solubilization of all antigens detectable with our antibody, except for ~20% of the 180-kD band (Fig. 6 A, lanes 11 and 12). Finally, extraction of nuclear envelopes with 0.1 N NaOH (Fig. 6 A, lanes 13 and 14) or 4 M guanidine-HCl (data not

3. In Fig. 6, only five of the RL1-immunoreactive polypeptides (bands of 180, 145, 100, 63, and 58 kD) were visible in the nuclear fractionation experiment (Fig. 6 A, lanes 1–3) and six of the polypeptides (bands of 210, 180, 145, 100, 63, and 58 kD) were visible in the nuclear envelope fractionation (Fig. 6 A, lanes 5–14), due to our inability to load substantially more antigen on SDS gels to visualize the most weakly reacting bands. When these immunoblots were overexposed, the 210-kD band was seen in Fig. 6 A, lanes 1–3 and the 54- and 45-kD bands were detectable in Fig. 6 A, lanes 5–14. These additional bands showed fractionation behavior very similar to the 100-kD band under all conditions examined (data not shown).

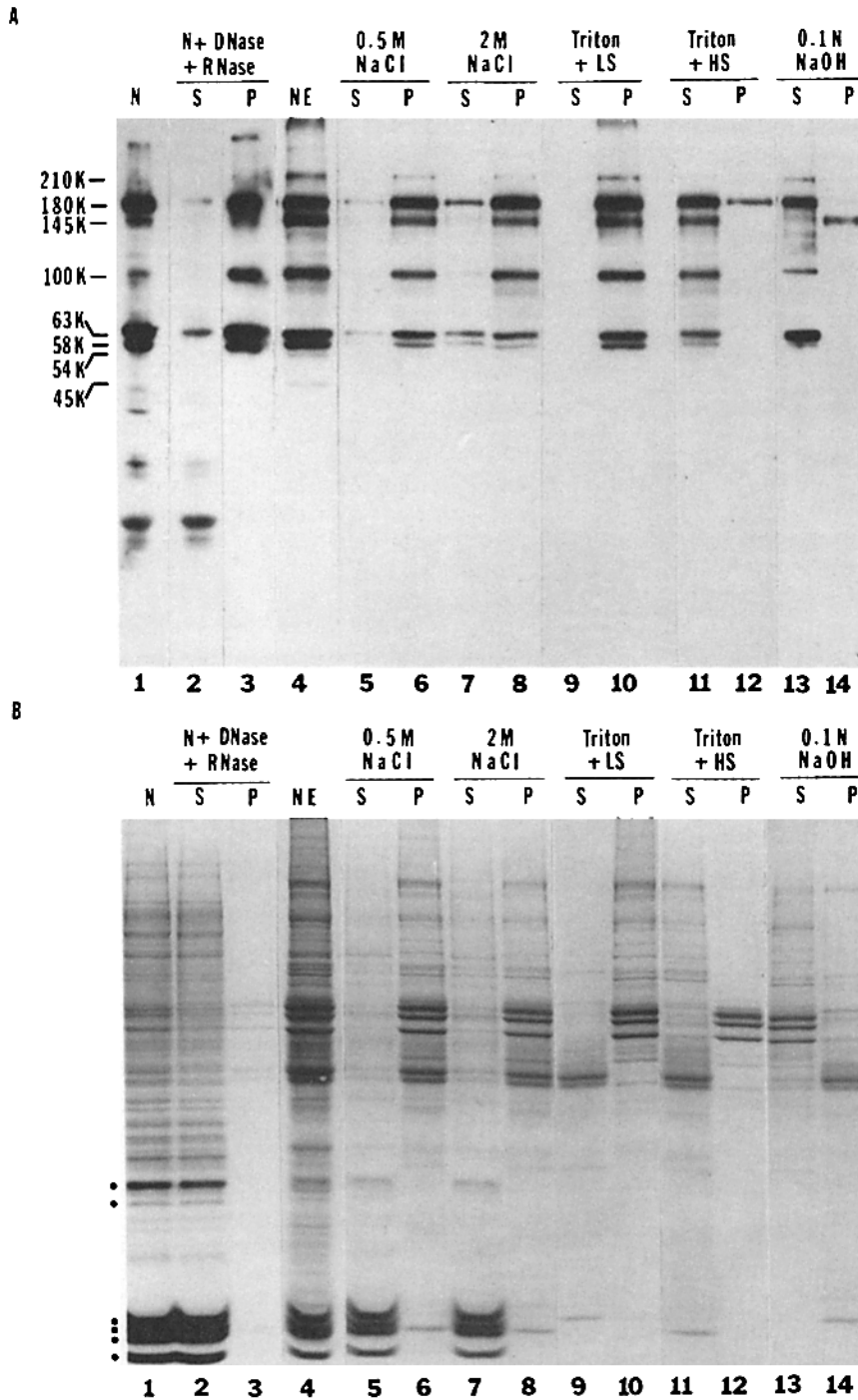


Figure 6. Behavior of the nuclear envelope antigens during subfractionation of nuclei and nuclear envelopes. Isolated rat liver nuclei (N) or nuclear envelopes (NE) were incubated with various extraction conditions as described in the text and Methods, and sedimented to yield insoluble pellets (P) and solubilized supernatants (S). Fractionated samples were analyzed by SDS gel electrophoresis followed by immunoblotting with RL1 (A, lanes 1-12), RL2 (A, lanes 13 and 14), or by staining with Coomassie Blue (B). 0.4 U of nuclei were analyzed in lanes 1-3, 2 U of crude nuclear envelopes were analyzed in lanes 4-8, and 2 U of 0.5 M NaCl-washed nuclear envelopes were analyzed in lanes 9-14. The labeled bands occurring in the 20-40-kD range of the nuclear samples (A, lanes 1 and 2) resulted from nonspecific antibody binding, since they were also labeled with an irrelevant mouse IgM (MS1; data not shown). Positions of the eight immunoreactive polypeptides are indicated to the left of A. Migration positions of molecular mass standards (numbers) and lamins A, B, and C are indicated to the right of B, and histones are indicated by dots to the left of B.

shown) to separate peripheral from integral membrane proteins (43) showed that most of the antigens are peripheral membrane proteins, and only the 145-kD band pellets with membrane vesicles as an integral membrane protein.

In summary, our fractionation data indicates that all eight polypeptides recognized by our antibodies are relatively tightly bound to nuclear envelopes, and that at least most of these polypeptides are highly enriched in the envelope fraction. The behavior of these antigens upon extraction of nuclear envelopes with nonionic detergent at various ionic strengths is consistent with a localization in the nuclear pore

complex, and is inconsistent with a tight association with the lamina or a localization in the outer nuclear membrane.

Punctate Immunofluorescence Labeling of Nuclei and Mitotic Cells

NRK cells were used for indirect immunofluorescence localization of the antigens recognized by our monoclonal antibodies (Fig. 7, A-D). Monoclonal antibodies RL1, RL2, RL3, RL4, RL6, and RL11 labeled the nucleus strongly in all interphase cells and gave a distinctive punctate labeling

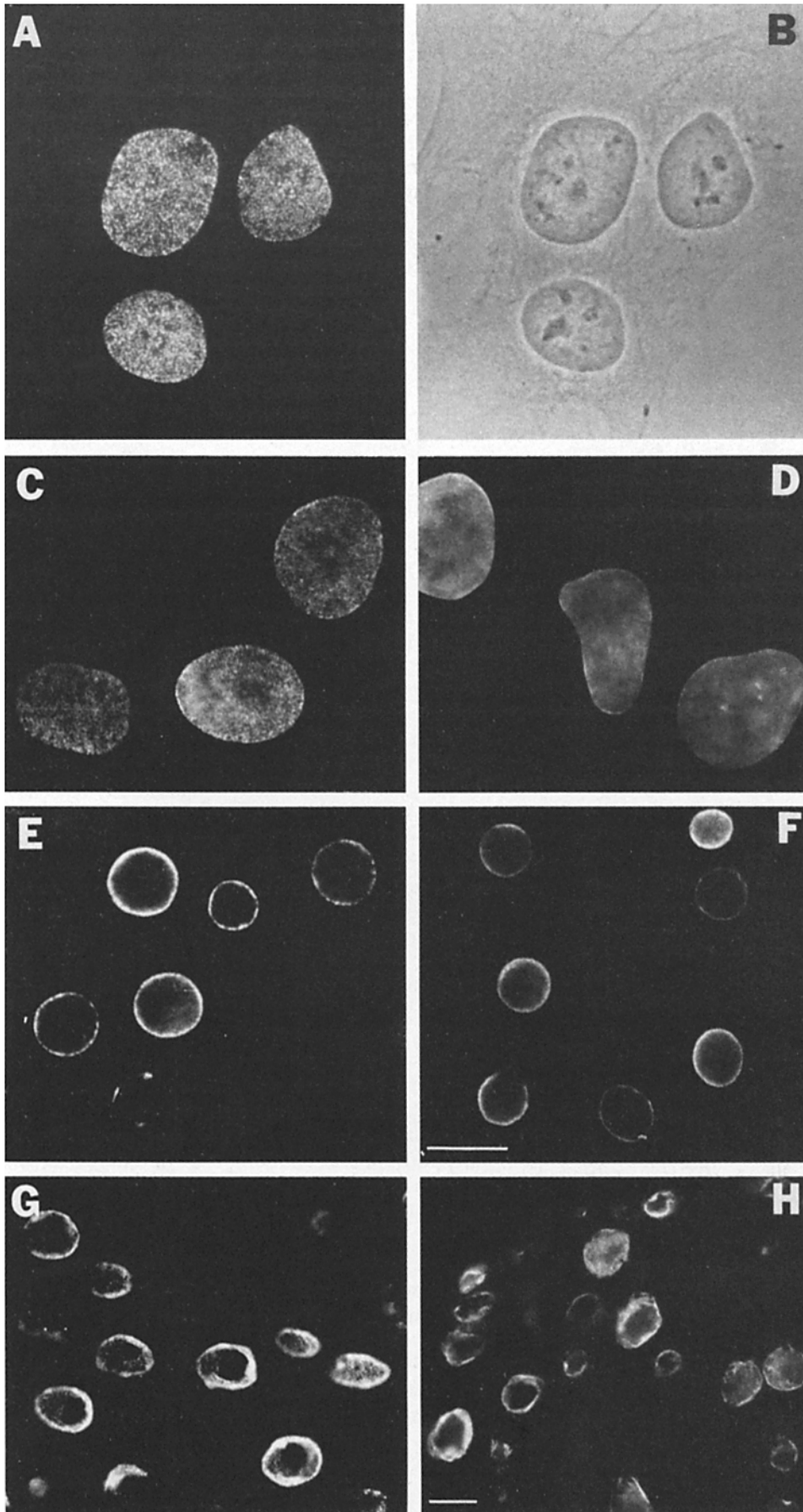


Figure 7. Immunofluorescence localization of the nuclear envelope antigens. (A-D) NRK cells were fixed for 4 min with 4% formaldehyde, permeabilized with Triton X-100, and labeled for indirect immunofluorescence microscopy with monoclonal antibodies RL1 (A; corresponding phase-contrast image shown in B), RL11 (C), and monoclonal antibody RL12 that is specific for the three nuclear lamins (D). (E-F) Isolated rat liver nuclei were centrifuged onto coverslips, fixed and permeabilized as described above, and labeled for immunofluorescence microscopy with RL1 (E) and RL12 (F). (G-H) 4- μ m thick cryosections were cut from rat liver, fixed with 100% methanol, and processed for immunofluorescence microscopy with RL1 (G) and RL12 (H). Bar, 10 μ m.

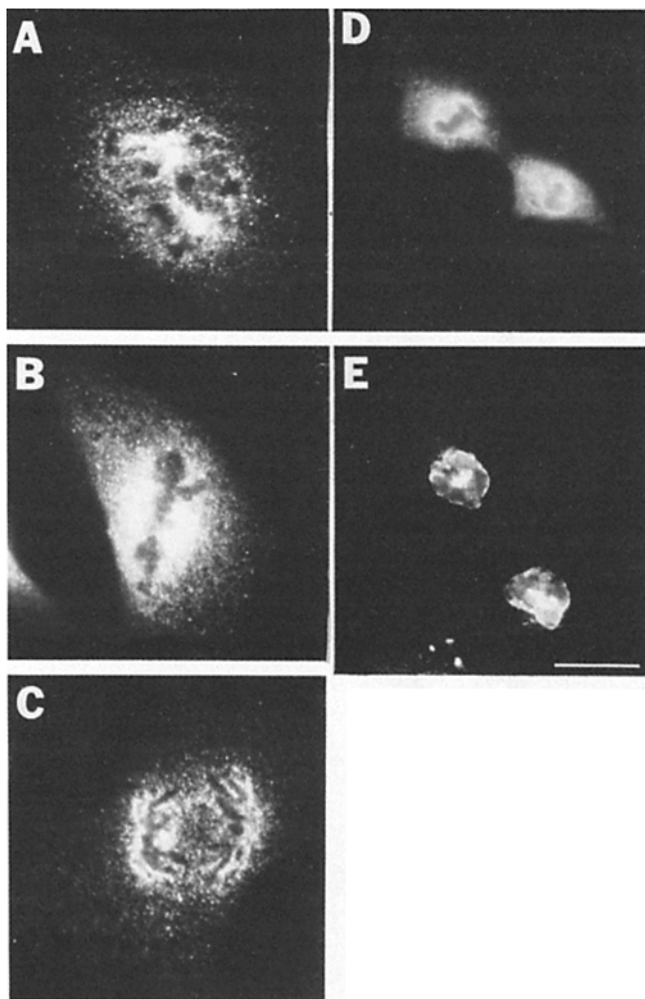


Figure 8. Immunofluorescence localization of the nuclear envelope antigens in mitotic cells. NRK cells were fixed for 10 min with 4% paraformaldehyde, permeabilized with Triton X-100, and labeled for indirect immunofluorescence microscopy with monoclonal antibody RL1. Shown are fluorescent images of cells in prometaphase (A), metaphase (B), late anaphase (C), telophase (D), and late telophase or early G1 (E). Bar, 10 μ m.

of the nuclear surface with little or no labeling of the cytoplasm (RL1 shown in Fig. 7, A and B, and RL11 shown in Fig. 7 C; others not shown). Since the nuclei of NRK cells are quite flat, it was possible to visualize a large area of the nuclear surface in a single focal plane. The punctate labeling of the nuclear surface obtained with these antibodies sharply contrasted with the more uniform nuclear surface labeling seen with a monoclonal antibody that recognizes the three nuclear lamins (Fig. 7 D; cf. to Fig. 7, A and C; see also references 18 and 34).

To analyze whether the antibodies exclusively label the nuclear surface or label the nuclear interior as well, isolated rat liver nuclei were examined by immunofluorescence microscopy. In contrast to nuclei in NRK cells, rat liver nuclei are round and allow clear-cut discrimination between nuclear surface vs. internal labeling in an appropriate focal plane. With these samples, the monoclonal antibodies strongly labeled the nuclear periphery and gave little or no staining of

the nuclear interior, although punctate labeling of the nuclear envelope was inconspicuous in most optical sections (RL1 shown in Fig. 7 E; others not shown). This peripheral labeling is identical to that seen for the nuclear lamins (Fig. 7 F) which are localized exclusively in the nuclear envelope. Analogous localization results were obtained by staining 4 μ m rat liver cryosections with RL1 (Fig. 7 G) and a monoclonal antibody reacting with the lamins (Fig. 7 H).

Thus, the results of immunofluorescence microscopy completely support our biochemical fractionation data, and indicate that the related antigens recognized by our monoclonal antibodies are specifically localized in the nuclear envelope. Furthermore, the punctate labeling pattern is strongly suggestive of a localization in the nuclear pore complex (see reference 5). Only one of the affinity-purified polyclonal antibodies that we prepared (anti-180 kD; see Fig. 4) gave a significant level of signal in immunofluorescence staining of NRK cells. In this case the staining pattern was identical to the punctate labeling obtained with the monoclonal antibodies (data not shown).

The nuclear lamins undergo reversible disassembly during mitosis (18, 34) coinciding with the disassembly and reformation of the nuclear envelope (14). Examination of NRK cells showed that the antigens labeled by monoclonal antibody RL1 undergo analogous changes during mitosis (Fig. 8). During prophase, the antigens were completely lost from the nuclear surface and by prometaphase (Fig. 8 A) had become dispersed throughout the cytoplasm. However, in marked contrast to the nuclear lamins that are homogeneously distributed throughout metaphase cells (18, 34), the disassembled RL1 antigens appeared as many tiny punctate foci. The antigens remained in this punctate disassembled state through metaphase (Fig. 8 B) and early to mid anaphase (data not shown). However, beginning in late anaphase (Fig. 8 C) and continuing in telophase (Fig. 8 D) the antigens reassociated with the chromosomal surfaces. By late telophase to early G1 (Fig. 8 E), the antigens were exclusively localized around the surfaces of the daughter chromosome sets.

Similar to the RL1 antigens, the proteins labeled by the other monoclonal antibodies were also reversibly disassembled to a dispersed punctate form in mitotic cells (data not shown). These results suggest that at least a substantial fraction of these antigens remain in discrete macromolecular structures after nuclear envelope disassembly. Nevertheless, it is plausible that some of the antigens are also uniformly distributed throughout mitotic cells like the lamins, but are not readily discernable by immunofluorescence microscopy in these cells.

EM Immunolocalization in the Pore Complex

We localized these antigens at the EM level by indirect immunogold labeling of isolated (non-detergent-treated) rat liver nuclear envelopes with monoclonal antibodies (Fig. 9). In many areas of these samples, it was possible to unambiguously distinguish outer and inner nuclear membranes, since the outer nuclear membrane was periodically ruptured and/or absent, while the inner membrane was mostly continuous (reference 7; see Fig. 9, E and G). With all antibodies tested (RL1, RL2, RL6, and RL11), labeling occurred exclusively at nuclear pore complexes (Fig. 9; e.g., arrow-

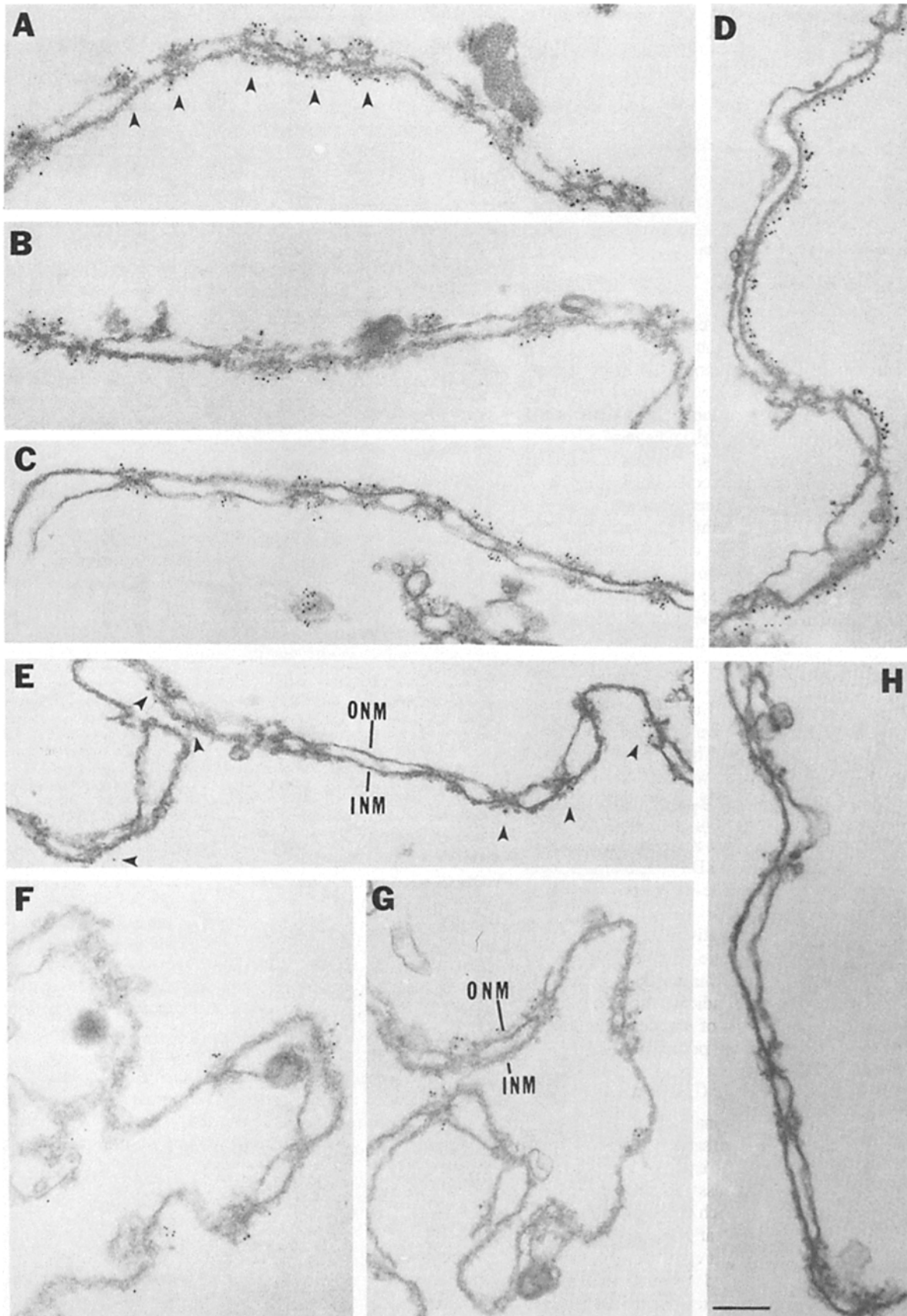


Figure 9. Immunoelectron microscopic localization of the nuclear envelope antigens in isolated rat liver nuclear envelopes. Isolated nuclear envelopes were washed with 0.5 M NaCl, fixed with paraformaldehyde, and incubated for indirect immunogold labeling with monoclonal antibodies RL1 (*A* and *B*), RL2 (*C*), monoclonal antibody RL12 that is specific for lamins (*D*), RL11 (*E* and *F*), RL6 (*G*), and an irrelevant

Table II. Quantitation of Gold Particles Bound to Cytoplasmic and Nucleoplasmic Sides of Pore Complexes in Antibody-labeled Nuclear Envelopes*

monoclonal antibody	No. pore complexes scored	No. gold particles counted	Gold on nucleoplasmic side	Gold on cytoplasmic side
			%	%
RL1	95	457	43	57
RL2	257	1,283	43	57
RL6	127	457	49	51
RL11	366	429	92	8

* Areas where the inner and outer nuclear membranes could be clearly distinguished were selected for analysis. Only gold-labeled pore complexes were scored.

heads in *A* and *E*) and was completely absent from other areas of nuclear membranes. Most labeling was seen at the cytoplasmic and/or nucleoplasmic margins of the pore complex in the regions of the eightfold symmetrical rings (see references 13 and 45). Little or no labeling in areas of the central radial spokes was seen, although it is conceivable that this region was relatively inaccessible to antibodies due to steric constraints. Furthermore, no specific labeling was ever seen on the luminal side of nuclear membranes (i.e., within the perinuclear space), even though this area was accessible to antibody labeling due to periodic discontinuities in the outer nuclear membrane. In contrast to this pattern, a monoclonal antibody recognizing the three lamins uniformly labeled the nucleoplasmic surface of the inner nuclear membrane (Fig. 9 *D*) and an irrelevant monoclonal IgG gave virtually no labeling of the nuclear envelope with our conditions (Fig. 9 *H*).

Antibodies RL1 (Fig. 9, *A* and *B*) and RL2 (Fig. 9 *C*), which recognize all eight nuclear envelope antigens, bound at high levels to all pore complexes. The nucleoplasmic and cytoplasmic margins of this structure were labeled to similar extents (Table II). Antibody RL6 (Fig. 9 *G*) also bound to both sides of the pore complex, although at lower levels than RL1 and RL2 (Table II). Interestingly, antibody RL11, which is virtually monospecific for the 180-kD band, bound almost exclusively to the nucleoplasmic side of the pore complex (Fig. 9, *E* and *F* and Table II).

In summary, all the monoclonal antibodies that we tested decorated exclusively the nuclear pore complex. Combined with the results of biochemical fractionation and immunofluorescence microscopy, these data indicate that most or all eight antigens recognized by our set of monoclonal antibodies occur specifically in the nuclear pore complex.

Abundance of Proteins in the Pore Complex

The antigens recognized by monoclonal antibody RL2 were immunoadsorbed quantitatively from samples of rat liver nuclear envelopes and the amount of each of the adsorbed bands was determined from Coomassie Blue-stained SDS gels, to estimate the abundance of each of the proteins in the pore complex (Table III). Between 5 and 13 ng of each polypeptide was measured in 1 U of nuclear envelopes (the amount derived from 3×10^6 nuclei). Based on these values, and assuming that 3.8×10^4 pore complexes occur in a rat liver

Table III. Quantities of Immunoreactive Polypeptides Present in Isolated Rat Liver Nuclear Envelopes*

Apparent molecular weight	ng/U†	Estimated molecules per pore complex‡
<i>kD</i>		
210	5.6 ± 0.82	1.7 ± 0.24
180	13.3 ± 0.90	4.7 ± 0.28
145	8.2 ± 0.90	3.6 ± 0.35
100	8.6 ± 1.0	5.4 ± 0.50
63	7.9 ± 1.6	7.9 ± 0.80
58	5.0 ± 1.4	5.4 ± 0.87
54	5.9 ± 0.74	6.8 ± 0.93
45	N.D.	N.D.
lamins A + B + C	1660 ± 254	—

* Antigens were immunoadsorbed from salt-washed nuclear envelopes with RL2 under conditions where all of the RL2 antigens detectable by immunoblotting with either RL2 or with specific polyclonal antibodies (Fig. 4) occurred in the antibody-bound fraction. Subsequently, samples were run on SDS gels and quantities of antigen were measured after staining with Coomassie Blue using bovine serum albumin as a standard. Values represent the average and standard deviations of three independent determinations.

† 1 U of nuclear envelopes is the amount of nuclear envelopes derived from 1 A_{260} U of isolated nuclei, which contains 3×10^6 nuclei. 1 U of salt-washed nuclear envelopes contains 7.3 ± 0.55 μ g protein ($n = 2$) as determined by the method of Lowry (37).

‡ Corrected for a 25% loss of nuclear envelope protein incurred during isolation of salt-washed nuclear envelopes from nuclei, as defined by the loss of the nuclear lamins during the same steps by quantitative immunoblotting measurements.

nucleus (39), we calculate that there are on average between two and eight copies of each polypeptide per pore complex (Table III), assuming that all eight polypeptides are present in every pore complex. A total of ~35 polypeptides of the group would occur in a single pore complex.

When association of radioactively labeled RL2 and RL11 with isolated nuclear envelopes was measured, saturable binding was obtained with both antibodies (Fig. 10). In a Scatchard plot (40), the RL2 binding showed a major class of sites (dotted line) with an apparent affinity of 5.3 nM present at 14.4 sites per pore complex. Additional lower affinity sites were also present. In a Scatchard plot of RL11 binding, a class of sites was seen at high antibody concentrations with an apparent affinity of 2.9 nM present at an average of 3.5 sites per pore complex. The number of binding sites per pore complex measured for RL2 and RL11 are consistent with the

monoclonal IgG HA4 (*H*). Examples of pore complexes (arrowheads in *A* and *E*) and the outer (*ONM*) and inner nuclear membranes (*INM*) are indicated. Bar, 180 nm.

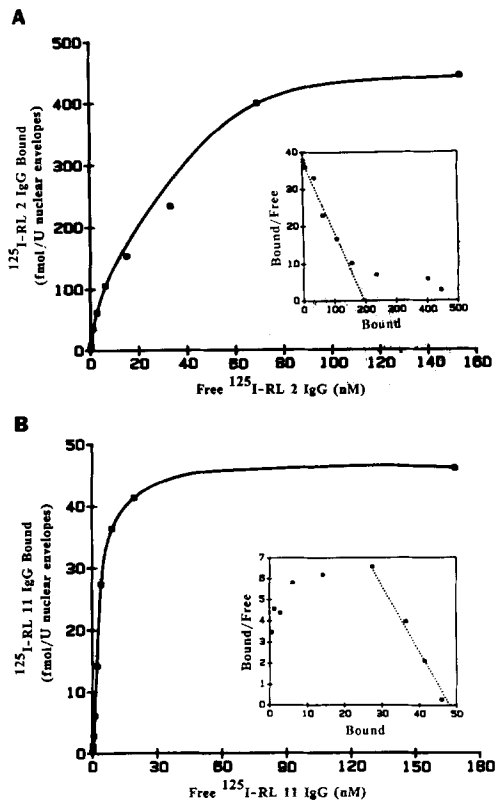


Figure 10. Binding of antibodies RL2 and RL11 to isolated rat liver nuclear envelopes. Rat liver nuclear envelopes that had been washed with 0.5 M NaCl were incubated with ^{125}I -labeled monoclonal antibodies RL2 (A) or RL11 (B) and amount of bound antibody was determined. Binding is expressed as fmol antibody bound per unit of salt-washed nuclear envelopes (containing $7.3 \pm 0.55 \mu\text{g}$ protein) minus values for nonspecific binding obtained with an irrelevant monoclonal IgG (HA4). Insets are Scatchard plots of the binding data (42), where Bound is the fmol bound antibody per unit of nuclear envelopes and Free is the concentration of unbound antibody. The dotted lines were drawn to define classes of high affinity binding sites. The plot of RL2 binding is consistent with negative cooperativity or the presence of multiple classes of binding sites, while that of RL11 is consistent with positive cooperativity.

relative levels of antibody decoration obtained by immunoelectron microscopy (Fig. 9). However, the number of binding sites measured by Scatchard analysis is likely to be an underestimate of the actual number of antigen molecules per pore complex (cf. Table III), because a single bivalent IgG molecule could bind to two antigen molecules, and stoichiometric binding of antibodies (particularly RL2) to all antigens in the pore complex could be sterically inhibited.

Discussion

A Novel Group of Pore Complex Glycoproteins

Using monoclonal antibodies, we identified a group of eight nuclear envelope polypeptides, migrating between 45 and 210 kD on SDS gels, which have common epitopes. Tryptic peptide mapping and immunoblotting with polyclonal antibodies showed that most or all of the eight polypeptides are structurally distinct. While the proteins are relatively tightly

bound to nuclear membranes, all are peripheral membrane proteins except for a 145-kD integral membrane protein. The eight polypeptides cofractionated with the pore complex under various conditions of ionic strength and nonionic detergent.

Immunofluorescence microscopy indicated that the eight antigens are highly enriched in the nuclear envelope, in agreement with the biochemical results. All of the monoclonal antibodies that were selected for this study gave distinctive punctate labeling of the nuclear surface, similar to the pattern recently described for a 62-kD polypeptide localized in the nuclear pore complex (5), and to the pattern obtained with monoclonal antibodies recognizing the pore complex glycoprotein gp190 (Senior, A., and L. Gerace, unpublished observation).

By immunoelectron microscopy performed on isolated rat liver nuclear envelopes, the four monoclonal antibodies we examined labeled exclusively the nuclear pore complex. These antibodies reacted with different subsets of the eight antigens on immunoblots, ranging from a single polypeptide (the 180-kD species) to all eight proteins. All of the polypeptides recognized on immunoblots by a particular monoclonal antibody may not have been labeled to the same relative extent in immunogold microscopy of intact nuclear envelopes. Nevertheless, it is probable that all eight polypeptides identified by our antibodies occur in the pore complex, considering the immunolocalization data together with the fractionation results.

With three of the four monoclonal antibodies, roughly equivalent levels of immunogold decoration were obtained on both the cytoplasmic and nucleoplasmic margins of the pore complex, concentrated in regions containing the eight-fold symmetrical rings (13, 45). In contrast, antibody RL11, which was virtually monospecific for the 180-kD band, labeled almost exclusively the nucleoplasmic side of the pore complex. This result raises the intriguing possibility that the 180-kD polypeptide, and perhaps other members of the group of eight antigens, occur exclusively on either one or the other side of the pore complex (see below). Our data do not distinguish whether all members of the antigen set are present in every pore complex, or whether certain proteins are restricted to a subset of the total pore complexes.

During mitosis, the proteins labeled by immunofluorescence microscopy were reversibly dispersed throughout the cytoplasm, coinciding with nuclear envelope disassembly and reformation. Interestingly, the antigens yielded a finely punctate staining pattern in metaphase and anaphase cells, suggesting that at least some of the eight polypeptides occur in discrete macromolecular complexes after nuclear envelope disassembly. These putative pore complex substructures may consist of functionally associated proteins.

As demonstrated in the accompanying paper (25), the group of nuclear envelope proteins identified by our monoclonal antibodies all contain a recently described protein glycosylation, O-linked *N*-acetylglucosamine (24, 44). Furthermore, this sugar modification forms a major part of the epitopes recognized by all of the monoclonal antibodies we have studied. Since the antibodies labeled only the cytoplasmic and nucleoplasmic (as opposed to luminal) surfaces of nuclear membranes in immunoelectron microscopy, this sugar modification necessarily must be disposed on the cytoplasmic and nucleoplasmic nuclear membrane surfaces. The

topological disposition of this protein-bound carbohydrate contrasts with that of other glycoprotein saccharide modifications that have been carefully analyzed in cells (e.g., asparagine-linked oligosaccharides, reference 32) which occur exclusively on the luminal side of intracellular membrane compartments.

The fact that multiple glycosylation sites are present on at least some of the eight pore complex proteins (see accompanying paper) could readily explain the observation that most of the monoclonal antibodies studied apparently recognize spatially separate epitopes on the 180-kD polypeptide. This could also account for the observation that different antibodies bind to different subsets of the group of eight proteins. It is likely that the 62-kD wheat germ agglutinin-binding glycoprotein recently localized in the pore complex (5) is identical to the 63-kD polypeptide reacting with our monoclonal antibodies, considering the similar biochemical properties of these two species.

Some of our monoclonal antibodies reacted weakly on immunoblots of nuclear envelopes with other bands, in addition to the eight polypeptides we have considered. These minor immunoreactive species may represent additional distinct members of the group of pore complex glycoproteins we have identified, although we did not analyze these proteins further because of their relatively low abundance. Interestingly, up to four additional polypeptides, similar in abundance to the major glycoproteins, appeared in samples immunoadsorbed from nuclear envelopes after solubilization with relatively nondenaturing conditions. These additional bands were completely unreactive with the monoclonal antibodies on immunoblots, and probably appeared in adsorbed samples due to a tight physical association with some of the glycoproteins. Thus, these coadsorbed polypeptides are good candidates for being additional pore complex components.

Based on its dimensions (13, 45), the pore complex may have a molecular mass of $25\text{--}50 \times 10^6$ D. If this is the case, then the group of pore complex glycoproteins we have identified, which comprises an estimated 3.5×10^6 D, would represent a relatively small fraction of the total mass (and probably number of proteins) of the pore complex.

Possible Functions of the Glycoproteins

We have detected polypeptides homologous to rat liver O-linked glycoproteins by immunofluorescence microscopy and immunoblotting in a variety of vertebrate cell types, including oocytes and cultured cells of *Xenopus laevis* (Senior, A., C. Featherstone, and L. Gerace, unpublished observation), and anticipate that their presence in the pore complex will be evolutionarily conserved. Since these O-linked glycoproteins occur at relatively low abundance (two to eight copies on average per pore complex), it is unlikely that they serve generalized structural functions, such as has been proposed for the pore complex glycoprotein gp190 (19), which is present at an estimated 25 copies per pore complex.

One intriguing possibility is that they constitute or are part of receptors for transporting different classes of macromolecules between nucleus and cytoplasm. Both their relative abundance (two to eight copies per pore) and their localization (in the peripheral rings of the pore complex facing the nucleoplasm and cytoplasm) are consistent with this possibility. An asymmetric localization in the pore complex (as sug-

gested for the 180-kD polypeptide) might be expected for such transport receptors, since translocation of many or all classes of large macromolecules across the pore complex may be a strictly vectorial process. Each pore complex could contain multiple distinct receptors on both its nucleoplasmic and cytoplasmic margins in the eightfold symmetrical rings, which could be connected to a common translocating machine(s) in the central regions of the pore. Whatever the actual functions of these glycoproteins, *in vivo* and *in vitro* functional analyses of the pore complex should be greatly facilitated with the information and immunological probes we have described in this paper.

We thank Dr. Brian Burke for extensive advice on production and use of monoclonal antibodies, and Ms. Mary Jean Meyer and Mr. Dave Gwynn for participating in hybridoma isolation. We are also grateful to Dr. Carol Featherstone and Dr. Frank Supryniewicz for insightful comments on the manuscript.

This work was supported by National Institutes of Health grant GM28521, American Cancer Society grant CD-280, and a Searle Scholars/Chicago Community Trust Award to L. Gerace.

Received for publication 24 November 1986, and in revised form 12 January 1987.

References

1. Aaronson, R., and G. Blobel. 1975. Isolation of nuclear pore complexes in association with a lamina. *Proc. Natl. Acad. Sci. USA.* 72:1007-1011.
2. Afzelius, B. 1955. The ultrastructure of the nuclear membrane of the sea urchin oocyte as studied with the electron microscope. *J. Cell Biol.* 8: 147-158.
3. Berrios, M., A. Filson, G. Blobel, and P. Fisher. 1983. A 174-kilodalton ATPase/dATPase and a glycoprotein of apparently identical molecular weight are common but distinct components of higher eukaryotic nuclear structural protein subfractions. *J. Biol. Chem.* 258:13384-13390.
4. Burke, B., G. Griffiths, H. Reggio, D. Louvard, and G. Warren. 1982. A monoclonal antibody against a 135-K Golgi membrane protein. *EMBO (Eur. Mol. Biol. Organ.) J.* 1:1621-1628.
5. Davis, L., and G. Blobel. 1986. Identification and characterization of a nuclear pore complex protein. *Cell.* 45:699-709.
6. Dingwall, C., S. Sharnick, and R. Laskey. 1982. A polypeptide domain that specifies migration of nucleoplasmin in the nucleus. *Cell.* 30:449-458.
7. Dingwall, C. 1985. The accumulation of proteins in the nucleus. *Trends Biochem. Sci.* 10:64-66.
8. Dwyer, N., and G. Blobel. 1976. A modified procedure for isolation of a pore complex-lamina fraction from rat liver nuclei. *J. Cell Biol.* 70:581-591.
9. Elder, J., R. Pickett, J. Hampton, and R. Lerner. 1977. Radioiodination of proteins in single polyacrylamide gel slices. *J. Biol. Chem.* 252: 6510-6515.
10. Feldherr, C., R. Cohen, and J. Ogburn. 1983. Evidence for mediated protein uptake by amphibian oocyte nuclei. *J. Cell Biol.* 96:1486-1490.
11. Feldherr, C., E. Kallenbach, and N. Schultz. 1984. Movement of a karyophilic protein through the nuclear pores of oocytes. *J. Cell Biol.* 99: 2216-2222.
12. Fenner, C., R. Traut, D. Mason, and J. Wilman-Coffelt. 1975. Quantification of Coomassie blue stained proteins in polyacrylamide gels based on analysis of eluted dye. *Anal. Biochem.* 63:595-602.
13. Franke, W., U. Scheer, G. Krohne, and E. Jarasch. 1981. The nuclear envelope and the architecture of the nuclear periphery. *J. Cell Biol.* 91: 39s-50s.
14. Fry, D. 1976. The nuclear envelope in mammalian cells. In *Mammalian Cell Membranes*, Vol. 2. G. Jamieson and D. Robinson, editors. Butterworth, Boston. pp. 197-265.
15. Gall, J. 1967. Octagonal pore complexes. *J. Cell Biol.* 32:391-399.
16. Gerace, L. 1987. Nuclear lamina and organization of nuclear architecture. *Trends Biochem. Sci.* In press.
17. Gerace, L., and G. Blobel. 1980. The nuclear envelope lamina is reversibly depolymerized during mitosis. *Cell.* 19:277-287.
18. Gerace, L., A. Blum, and G. Blobel. 1978. Immunocytochemical localization of the major polypeptides of the nuclear pore complex-lamina fraction. *J. Cell Biol.* 79:546-566.
19. Gerace, L., Y. Ottaviano, and C. Kondor-Koch. 1982. Identification of a major polypeptide of the nuclear pore complex. *J. Cell Biol.* 95:826-837.
20. Gerace, L., C. Comeau, and M. Benson. 1984. Organization and modulation of nuclear lamina structure. *J. Cell Sci.* 1(Suppl.):137-160.

21. Goldfarb, D., J. Garipey, G. Schoolnik, and R. Kornberg. 1986. Synthetic peptides as nuclear localization signals. *Nature (Lond.)* 322:641-644.
22. Greenwood, F., W. Hunter, and J. Glover. 1963. The preparation of ¹³¹I-labelled human growth hormone of high specific radioactivity. *Biochem. J.* 89:114-123.
23. Hall, M., L. Hereford, and I. Herskowitz. 1984. Targeting of E. coli β -galactosidase to the nucleus in yeast. *Cell* 36:1057-1065.
24. Holt, G., and G. Hart. 1986. The subcellular distribution of terminal N-acetylglucosamine moieties. *J. Biol. Chem.* 261:8049-8057.
25. Holt, G., C. Snow, A. Senior, R. Haltiwanger, L. Gerace, and G. Hart. 1987. Nuclear pore complex glycoproteins contain cytoplasmically disposed O-linked N-acetylglucosamine. *J. Cell Biol.* 104:1157-1164.
26. Hubbard, A., and A. Ma. 1983. Isolation of rat hepatocyte plasma membranes. II. Identification of membrane-associated cytoskeletal proteins. *J. Cell Biol.* 96:230-239.
27. Hubbard, A., J. Bartles, and L. Braiterman. 1985. Identification of rat hepatocyte plasma membrane proteins using monoclonal antibodies. *J. Cell Biol.* 100:1115-1125.
28. Kalderon, D., B. Roberts, W. Richardson, and A. Smith. 1984. A short amino acid sequence able to specify nuclear location. *Cell* 39:499-509.
29. Kay, R., D. Fraser, and I. Johnston. 1972. A method for the rapid isolation of nuclear membranes from rat liver. *Eur. J. Biochem.* 30:145-154.
30. Kearney, J., A. Radbruch, B. Liesegang, and K. Rajewsky. 1979. A new mouse myeloma cell line that has lost immunoglobulin expression but permits the construction of antibody-secreting hybrid lines. *J. Immunol.* 123:1548-1550.
31. Kiehart, D., D. Kaiser, and T. Pollard. 1984. Monoclonal antibodies demonstrate limited structural homology between myosin isozymes from *Acanthamoeba*. *J. Cell Biol.* 99:1002-1014.
32. Kornfeld, R., and S. Kornfeld. 1985. Assembly of asparagine-linked oligosaccharides. *Annu. Rev. Biochem.* 54:631-664.
33. Krohne, G., and R. Benavente. 1986. The nuclear lamins. A multigene family of proteins in evolution and differentiation. *Exp. Cell Res.* 162:1-10.
34. Krohne, G., W. Franke, S. Ely, A. D'Arcy, and E. Jost. 1978. Localization of a nuclear envelope-associated protein by indirect immunofluorescence microscopy using antibodies against a major polypeptide from rat liver fractions enriched in nuclear envelope associated material. *Cyobiologie.* 18:22-38.
35. Lang, I., M. Scholz, and R. Peters. 1986. Molecular mobility and nucleocytoplasmic flux in hepatoma cells. *J. Cell Biol.* 102:1183-1190.
36. Lanford, R., P. Kanda, and R. Kennedy. 1986. Induction of nuclear transport with a synthetic peptide homologous to the SV40 T antigen transport signal. *Cell* 46:575-582.
37. Lowry, O., N. Rosebrough, A. Farr, and R. Randall. 1951. Protein measurement with the Folin phenol reagent. *J. Biol. Chem.* 193:265-275.
38. Maizel, J. 1969. Acrylamide gel electrophoresis of proteins and nucleic acids. In *Fundamental Techniques in Virology*. K. Habel and N. Salzman, editors. Academic Press, Inc., New York. pp. 334-362.
39. Maul, G. 1977. The nuclear and cytoplasmic pore complex. Structure, dynamics, distribution and evolution. *Int. Rev. Cytol.* 6(Suppl.):76-186.
40. Ottaviano, Y., and L. Gerace. 1985. Phosphorylation of the nuclear lamins during interphase and mitosis. *J. Biol. Chem.* 260:624-632.
41. Paine, P., L. Moore, and S. Horowitz. 1975. Nuclear envelope permeability. *Nature (Lond.)* 254:109-114.
42. Scatchard, G. 1949. The attraction of proteins for small molecules and ions. *Ann. N.Y. Acad. Sci.* 51:660-672.
43. Steck, T., and J. Yu. 1973. Selective solubilization of proteins from red blood cell membranes by protein perturbants. *J. Supramol. Struct.* 1:220-231.
44. Torres, C., and G. Hart. 1984. Topography and polypeptide distribution of terminal N-acetylglucosamine residues on the surfaces of intact lymphocytes. *J. Biol. Chem.* 259:3308-3317.
45. Unwin, N., and R. Milligan. 1982. A large particle associated with the perimeter of the nuclear pore complex. *J. Cell Biol.* 93:63-75.
46. Warren, G., J. Davoust, and A. Cockcroft. 1984. Recycling of transferrin receptors in A431 cells inhibited during mitosis. *EMBO (Eur. Mol. Biol. Organ.) J.* 3:2217-2225.
47. Williams, C., and M. Chase. 1967. *Methods Immunol. Immunochem.* 1:307-385.